RSC Advances

COMMUNICATION

View Article Online
View Journal | View Issue

Conjugated anthracene dendrimers with monomer-like fluorescence†

Cite this: *RSC Adv.*, 2014, **4**, 19846

Received 17th March 2014
Accepted 8th April 2014

DOI: 10.1039/c4ra02341b

www.rsc.org/advances

Karl Börjesson,[a] Mélina Gilbert,[b] Damir Dzebo,[b] Bo Albinsson[b] and Kasper Moth-Poulsen*[a]

Two generations of highly emissive conjugated anthracene dendrimers containing up to 9 anthracene units are presented. In these dendrimers, anthracene-like absorption and emission properties are preserved due to the relatively weak electronic coupling between the anthracene units, while evidence of fast crosstalk within the molecular framework is still observed.

Developing materials containing photoactive units in a dendritic fashion has gained much interest in the last decade due to their attractive physical properties for molecular electronics.[1–6] Compared to linear conjugated polymers, dendrimers offer several advantages. They generally have higher solubility and hence are more solution-processable. Their three-dimensional structure prevents aromatic stacking interactions to occur, and thus decrease tendencies of aggregate formation.[7–12] For solid-state devices, incorporating emitter molecules in dendritic structures, apart from increasing the solution processability, also replaces the need of strong intermolecular coupling with an intramolecular one.

From a photophysical point of view, multichromophoric dendrimers, due to their well-defined structure, are also excellent model systems for investigating electron and energy transfer processes. Several examples of dendrimers functionalized with chromophoric groups showing intramolecular energy and charge migration have been reported.[13–17] For instance, Hofkens and co-workers have examined electronic communication between structurally identical chromophores. In particular by combining both time-resolved fluorescence anisotropy and single-molecule spectroscopy, they resolved both temporally and spatially energy transfer processes between peryleneimide chromophores in rigid polyphenylene dendrimers.[18] Other examples of dendrimers showing intramolecular energy transfer between dendrons have been reported by the groups of Meijer[19] and Goodson.[17,20,21]

Recently dendrimers containing up to three anthracenes have been prepared displaying interesting photophysical properties such as blue, green and white emission.[22–29] In this communication, two generations of highly emissive conjugated anthracene dendrimers, containing up to nine anthracene units, are reported (Scheme 1). The dendrimers only consist of sp^2 hybridized carbons in the form of diphenylanthracene, forming a conjugated and rigid structure that without the need

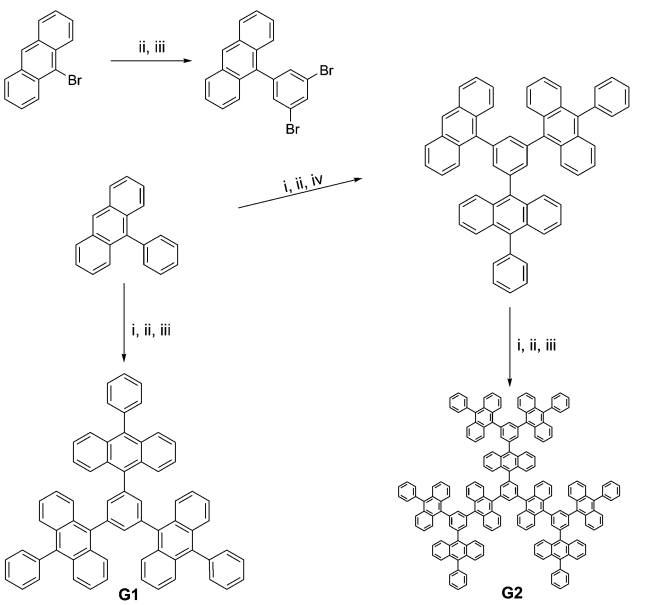

Scheme 1 (i) Br_2, CCl_4, 0 °C; (ii) (a) *tert*-butyllithium, THF, −78 °C; (b) 2-isopropoxy-4,4,5,5-tetramethyl-1,3,2-dioxaborolane, THF, −78 °C to 0 °C; (iii) $Pd_2(dba)_3$, TEAOH, tri(*o*-tolyl)phosphine, 1,3,5-tribromobenzene, toluene, reflux; (iv) $Pd_2(dba)_3$, TEAOH, tri(*o*-tolyl) phosphine, 1-anthracene-3,5-dibromobenzene, toluene, reflux.

[a]*Department of Chemical and Biological Engineering/Applied Chemistry, Chalmers University of Technology, 412 96 Göteborg, Sweden. E-mail: kasper.moth-poulsen@chalmers.se*

[b]*Department of Chemical and Biological Engineering/Physical Chemistry, Chalmers University of Technology, 412 96 Göteborg, Sweden*

† Electronic supplementary information (ESI) available: Experimental details of synthesis and spectroscopy; analysis of exciton model, quantum mechanical calculations and estimation of FRET rates. See DOI: 10.1039/c4ra02341b

of solubilizing aliphatic side chains, is soluble in common organic solvents. Their photophysical properties are compared with 9,10-diphenylanthracene (DPA) which emits blue light at a close to unity quantum yield.[30] In the vast majority of multi-chromophoric conjugated polymers, chromophore–chromophore interactions lead to red-shifted absorption and lower fluorescence quantum yields, thus altering their photophysical properties compared to the monomers. Our dendrimer system demonstrates that, with proper electronic coupling between the constituents, the excited state can be partially delocalized with fast exciton diffusion within the molecule while the attractive absorption and emission properties of the monomeric unit are retained.

The two nearly C3 symmetric dendrimers consist of 3 (G1) and 9 (G2) anthracene units respectively. They are made by a convergent synthetic approach, using 1,3,5-tribromobenzene as the core unit to produce the symmetric dendrimers from dendron arms (Scheme 1, for synthetic procedures see ESI†). This method enables separation of the dendron arms and not fully functionalized cores from the product, producing dendrimers of high purity.[31–33] The dendrons are synthesized from benzenes and anthracenes, with the key synthetic step being the introduction of a bromide functionality at the 9 position of anthracene. This reaction is surprisingly selective using 1 eq. of bromine at 0 °C. The yield of the reaction is close to quantitative, and it does not seem to be very concentration dependent (*vide infra*). The brominated anthracene is transformed to the corresponding boronic ester by lithiation followed by boronic esterification. This reaction produces boronic esters in high yields but works best at quite high concentrations (~90 mM). The boronic ester of the dendron is coupled using palladium chemistry with 1,3,5-tribromobenzene or 1-anthracene-3,5-bromobenzene to produce the dendrimer or one generation higher dendron, respectively. This is also a reaction that gives the best result when performed at high concentrations (~20 mM).

When the dendron grows the mass solubility is more or less retained, however, the molar solubility is not. This forces the reactions to be performed in more dilute solutions, with longer reaction times and dryer solvent requirements. All three reaction types retain their selectivity when performed in diluted solutions, but their sensitivity towards oxygen increases. This is seen as an increased fraction of dendrons having lost their boronic ester in the reaction mixture (loss of ester functionality is the only detected side product in this reaction). So even though the limit of how large this family of dendrimers can be has not been reached here, it is probably solubility rather than selectivity issue that will determine the practical size limit. Still the solubility of G2 is high enough (solubility > 5 mg ml^{-1} in toluene) for solution processing in molecular electronics applications.

Despite the different size of their conjugated system, the three compared molecules (DPA, G1 and G2) show similar spectral properties. Fig. 1 compares the absorption and emission spectra of the dendrimers and DPA. Only small changes in the ratio of the intensities of the vibronic peaks, and a minor red shift of the 0–0 transition energy level (E_{0-0} located at 401, 405 and 408 nm for DPA, G1 and G2 respectively) are observed.

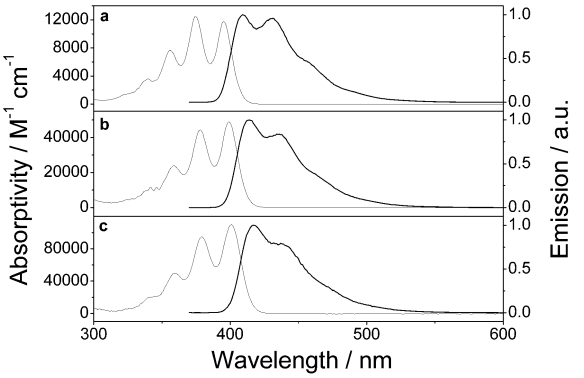

Fig. 1 Absorption and emission (excited at 354 nm) spectra of DPA (a), G1 (b) and G2 (c) dissolved in toluene.

The fluorescence quantum yields in toluene of G1 and G2 are close to unity, which is similar to DPA (Table S1†). Fluorescence emission of both dendrimers decays mono-exponentially and faster than for DPA, indicative of a higher radiative rate constants for G1 and G2 (Fig. S1 and Table S1†). Prolonged photolysis also reveals that the dendrimers are, due to their larger radiative rate constant, more photochemically stable than DPA (Fig. S2 and S3†).

One challenge in dendritic structures is to understand how electronic communication between the different dendrons occurs. Two extreme cases for electronic communication within the dendrimers can be distinguished. In the first case, the excitation energy is initially localized on one DPA unit and subsequently migrates by hopping to other DPA chromophores. The second case is a fully delocalized model where excitation energy is directly delocalized on the whole dendrimer upon excitation (see Fig. S4–S6† for visualization). Here the similar spectral properties of the dendrimers and the monomer suggest a relatively weak electronic coupling among the DPA moieties in G1 and G2, and favors an exciton located on individual anthracene moieties. The existence of a weak coupling is also supported by semi-empirical calculations (INDO/S) of the oscillator strengths (Fig. S7†), which show a linear increase of the oscillator strength from DPA to G1 to G2 as the chromophore gets larger. However the faster radiative rate constants of the dendrimers indicate a more cooperative excitation and emission of the individual DPA units (radiative coupling) and points towards at least a partially delocalized exciton.[34]

In order to investigate how localized or delocalized the exciton is in the dendrimers, fluorescence anisotropy experiments were performed (Fig. 2 and S8†). At 100 K, DPA has, as reported previously,[35] an increasing anisotropy with increasing excitation wavelength over the lowest absorption band reaching a value close to 0.4 at the red-edge of the absorption, indicating that the transition dipoles responsible for the absorption and emission events are close to collinear.[36] G1 and G2, however, exhibit a much more structured (and interesting) anisotropy profile. The anisotropy is lower and oscillates, with the maxima of the peaks off resonance with the vibronic peaks seen in the absorption spectra (Fig. 2). The amplitude of the oscillation is

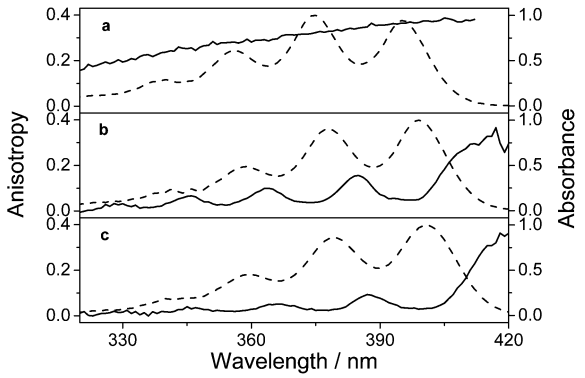

Fig. 2 Absorption (dashed lines) and steady-state fluorescence excitation anisotropy (solid lines) of DPA (a), G1 (b) and G2 (c) in 2-MTHF at 100 K.

larger in G1 than G2, which has the lowest anisotropy of the three molecules.

To interpret these oscillations in anisotropy, a fully delocalized exciton model is considered.[37] For G1, this would give rise to three transitions, one forbidden at high energy, and the other two at lower energy being degenerate and perpendicular to each other (Fig. S5 and S6†). By considering these two major perpendicular transitions and assuming for one of them a limiting anisotropy of 0.3 (the maximum observed value of the anisotropy for G1), the absorption spectra associated to these two electronic transitions are resolved with the help of the fluorescence excitation anisotropy (Fig. 3; for details see ESI†).[38] The degeneracy of the lowest electronic transitions is lifted probably due to static and dynamic distortions of the dendrimer geometry. The energy splitting between the two transitions is estimated from the resolved absorption spectra to 250 cm^{-1}. Thus, anisotropy oscillations in G1 can be attributed to the presence of two nearly degenerate transitions and point towards a delocalization of the exciton. INDO/S calculations of AM1 optimized structures (Fig. S7†) of the dendrimers confirm the presence of two nearly degenerate equally strong (oscillator strength of 0.7) electronic transitions constituting the lowest absorption band of G1. For G2, despite the increased number of combinations of the transition dipole moments to be considered, explanation of the anisotropy oscillations by the presence of several nearly degenerate transitions seems to prevail as well.

Further evidence on the electronic communication in the dendrimers comes from time-resolved anisotropy measurements. Both temperature-dependent and excitation wavelength-dependent anisotropy decays of G1 and G2 were measured and compared to the ones of DPA. At room temperature, the anisotropies decay mono-exponentially with a gradual increase of the correlation time from DPA *via* G1 to G2, which can be attributed to the rotational motion of the chromophores. Also no excitation wavelength dependency of the anisotropy decay is observed at room temperature. When the temperature is lowered, the correlation time gets, as expected, longer due to the increased viscosity of the solvent that slows down the rotation of the molecules (Table S2 and Fig. S9†). More interestingly for G1 at intermediate temperatures (160 K and 140 K), when the sample was excited at 385 nm and 395 nm, corresponding to high and low fundamental anisotropy values respectively, two correlation times were necessary to fit the anisotropy decays (Fig. 4).

While the anisotropy decay measured at 385 nm shows an initial fast decay, the anisotropy decay measured at 395 nm exhibits a corresponding rise time, and subsequently a slow decay as for 385 nm (Table 1). The long correlation time agrees well with our estimation of rotational correlation time (Table S2†), while the short lifetime suggests the presence of two non-degenerate emitting states. Excitation at 385 nm initially populates the lowest excited state with high anisotropy while the excited state with higher energy and low anisotropy is mainly populated when exciting at 395 nm (Fig. 3). This agrees well with our interpretation of the oscillating steady-state anisotropy for G1 originating from the presence of two nearly degenerate transitions. However, this short lifetime ($\approx$0.5 ns at 160 K) is relatively long compared to the times expected for internal conversion (1 ps or less) or excitation energy transfer

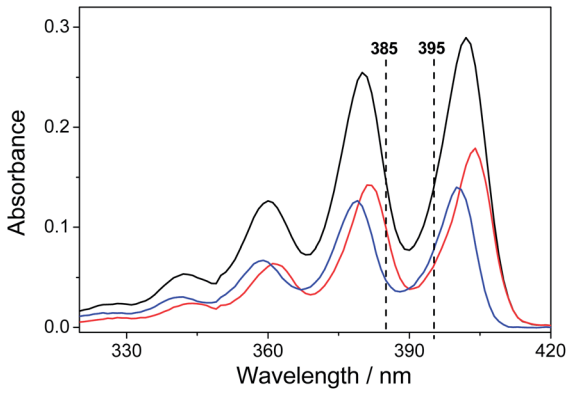

Fig. 3 Absorption (black) and resolved spectral components (blue and red) of the lowest absorption band in G1. The dashed lines indicate the excitation wavelengths chosen for time-resolved anisotropy measurements (approximately at the local max and min of the excitation anisotropy (*cf.* Fig. 2b)).

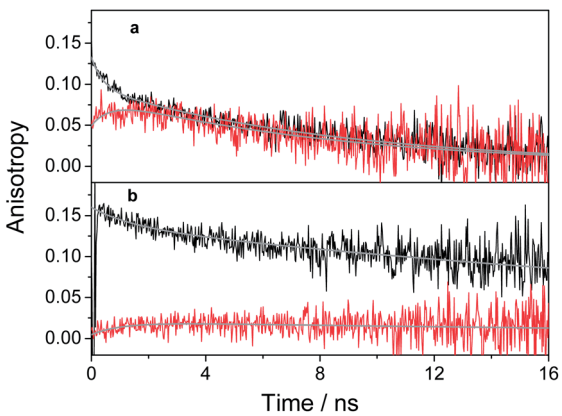

Fig. 4 Time-resolved fluorescence anisotropy decays of G1 at (a) 160 K and (b) 140 K, excited at 385 nm (black) and at 395 nm (red). Solid gray lines show fits to a bi-exponential model and the fitting parameters are summarized in Table 1.

Table 1 Fitted fluorescence anisotropy decay parameters of G1 in 2-MTHF as function of excitation wavelength and temperature

T (K)	λ_{exc} (nm)	$r_{0,a}$	θ_a (ns)	$r_{0,b}$	θ_b (ns)	χ^2
160	385	0.04	0.42	0.09	8.6	1.516
	395	−0.04	0.66	0.09	8.6	0.879
140	385	0.02	1.5	0.14	34	1.187
	395	−0.02	1.04	0.02	34	0.973

processes. A rough estimation of the minimum excitation energy transfer (EET) rate in G1 using the FRET model gives a transfer rate of 10^{13} s^{-1} and a EET time of 100 fs (more details in the ESI†). Thus, the observed short correlation time of the order 0.5 ns is unlikely to reflect excitation energy migration but instead can be interpreted as the time to reach equilibrium between the two emitting states. The fact that this equilibrium is slow despite the small energy difference between the two emitting states can be explained by one of the reactions being uphill in energy. As we further decrease the temperature to 140 K, both the short correlation times (rise and decay) become longer. The change with temperature is consistent with Arrhenius activation energy of roughly 250 cm^{-1}, supporting the interpretation of these decay times as the time to reach equilibrium between the two nearly degenerate lowest electronic transitions. At 80 or 100 K (Fig. S10†), the upward rate is predicted to be too slow to be observed during the excited state lifetime. This corresponds to a system that undergoes the normal fast internal conversion to the lowest excited state and emitting from this state alone, leading to the oscillatory behavior of the steady state anisotropy when varying the excitation wavelength (Fig. 2).

Thus, time-resolved anisotropy measurements did not permit to resolve any excitation energy migration processes in the dendrimers. But it is noteworthy that the r_0 values obtained from the fitted anisotropy decays are much lower for G1 and G2 than for DPA (Table 1 and S2†). This feature confirms the presence of an additional ultrafast depolarization channel in G1 and G2 that can be interpreted as excitation energy migration among DPA moieties. This process seems to be too fast to be resolved by TCSPC whose time resolution is about 25 ps. In an attempt to resolve excitation energy migration, the first ns of the fluorescence anisotropy decays were also measured using a streak camera system with a time resolution in the order of 10 ps, but this time resolution was still too low to observe any energy transfer processes. Future work will explore possibilities to resolve excitation energy migration in these dendritic structures using femtosecond pulsed excitation exploring both absorption anisotropy and singlet–singlet annihilation at high excitation fluencies.

Conclusions

In summary, two generations of highly emissive conjugated dendrimers, based on diphenylanthracene, have been synthesized using a simple and versatile chemical reactions sequence. These highly soluble systems show an absorption and emission envelope very similar to 9,10-diphenylanthracene, as well as a fluorescence quantum yield close to unity. Based on the photophysical measurement and theoretical framework presented here we conclude that the excited state in the dendrimers is at least partially delocalized and the partially delocalized exciton migrates within the conjugated structure faster than a few ps. These dendrimers illustrate the fact that it is possible to make highly soluble, conjugated molecules where the electronic coupling between its sub units is low enough to retain monomer-like absorption and emission properties, but still high enough to exhibit an extremely fast crosstalk within the molecular framework.

Acknowledgements

The authors would wish to acknowledge Victor Gray for determining melting points on the dendrimers.

Notes and references

1 A. Adronov and J. M. J. Frechet, *Chem. Commun.*, 2000, 1701–1710.
2 A. Mishra, C. Q. Ma, R. A. J. Janssen and P. Bauerle, *Chem.–Eur. J.*, 2009, **15**, 13521–13534.
3 S.-C. Lo and P. L. Burn, *Chem. Rev.*, 2007, **107**, 1097–1116.
4 J. H. Huang, J. H. Su and H. Tian, *J. Mater. Chem.*, 2012, **22**, 10977–10989.
5 C.-H. Wu, C.-H. Chien, F.-M. Hsu, P.-I. Shih and C.-F. Shu, *J. Mater. Chem.*, 2009, **19**, 1464–1470.
6 S. Q. Zhuang, R. G. Shangguan, J. J. Jin, G. L. Tu, L. Wang, J. S. Chen, D. G. Ma and X. J. Zhu, *Org. Electron.*, 2012, **13**, 3050–3059.
7 T. S. Qin, J. Q. Ding, M. Baumgarten, L. X. Wang and K. Müllen, *Macromol. Rapid Commun.*, 2012, **33**, 1036–1041.
8 T. S. Qin, J. Q. Ding, L. X. Wang, M. Baumgarten, G. Zhou and K. Müllen, *J. Am. Chem. Soc.*, 2009, **131**, 14329–14336.
9 M. R. Zhu, J. H. Zou, S. J. Hu, C. G. Li, C. L. Yang, H. B. Wu, J. G. Qin and Y. Cao, *J. Mater. Chem.*, 2012, **22**, 361–366.
10 M. C. Tang, D. P. K. Tsang, M. M. Y. Chan, K. M. C. Wong and V. W. W. Yam, *Angew. Chem., Int. Ed.*, 2013, **52**, 446–449.
11 P. W. Wang, Y. J. Liu, C. Devadoss, P. Bharathi and J. S. Moore, *Adv. Mater.*, 1996, **8**, 237–241.
12 P. Moonsin, N. Prachumrak, S. Namuangruk, S. Jungsuttiwong, T. Keawin, T. Sudyoadsuk and V. Promarak, *Chem. Commun.*, 2013, **49**, 6388–6390.
13 D. Turp, T. T. T. Nguyen, M. Baumgarten and K. Müllen, *New J. Chem.*, 2012, **36**, 282–298.
14 S. L. Gilat, A. Adronov and J. M. J. Frechet, *Angew. Chem., Int. Ed.*, 1999, **38**, 1422–1427.
15 C. Devadoss, P. Bharathi and J. S. Moore, *J. Am. Chem. Soc.*, 1996, **118**, 9635–9644.
16 M. Takahashi, H. Morimoto, K. Miyake, M. Yamashita, H. Kawai, Y. Sei and K. Yamaguchi, *Chem. Commun.*, 2006, 3084–3086.
17 J. Zhang, M. K. R. Fischer, P. Bauerle and T. Goodson, *J. Phys. Chem. B*, 2013, **117**, 4204–4215.

18 F. C. De Schryver, T. Vosch, M. Cotlet, M. Van der Auweraer, K. Mullen and J. Hofkens, *Acc. Chem. Res.*, 2005, **38**, 514–522.
19 S. C. J. Meskers, M. Bender, J. Hubner, Y. V. Romanovskii, M. Oestreich, A. Schenning, E. W. Meijer and H. Bassler, *J. Phys. Chem. A*, 2001, **105**, 10220–10229.
20 G. Ramakrishna, A. Bhaskar, P. Bauerle and T. Goodson, *J. Phys. Chem. A*, 2008, **112**, 2018–2026.
21 O. P. Varnavski, J. C. Ostrowski, L. Sukhomlinova, R. J. Twieg, G. C. Bazan and T. Goodson, *J. Am. Chem. Soc.*, 2002, **124**, 1736–1743.
22 J.-Y. Hu, Y.-J. Pu, Y. Yamashita, F. Satoh, S. Kawata, H. Katagiri, H. Sasabe and J. Kido, *J. Mater. Chem. C*, 2013, **1**, 3871–3978.
23 L. Wang, W. Y. Wong, M. F. Lin, W. K. Wong, K. W. Cheah, H. L. Tam and C. H. Chen, *J. Mater. Chem.*, 2008, **18**, 4529–4536.
24 J. H. Huang, B. Xu, J. H. Su, C. H. Chen and H. Tian, *Tetrahedron*, 2010, **66**, 7577–7582.
25 H. Huang, Q. Fu, S. Q. Zhuang, G. Y. Mu, L. Wang, J. S. Chen, D. G. Ma and C. L. Yang, *Org. Electron.*, 2011, **12**, 1716–1723.
26 B. L. Dong, M. L. Wang, C. X. Xu, Q. Feng and Y. Wang, *Cryst. Growth Des.*, 2012, **12**, 5986–5993.
27 J. C. Ribierre, A. Ruseckas, H. Cavaye, H. S. Barcena, P. L. Burn and I. D. W. Samuelt, *J. Phys. Chem. A*, 2011, **115**, 7401–7405.
28 G. Bergamini, P. Ceroni, P. Fabbrizi and S. Cicchi, *Chem. Commun.*, 2011, **47**, 12780–12782.
29 H. Huang, Q. A. Fu, S. Q. Zhuang, Y. K. Liu, L. Wang, J. S. Chen, D. G. Ma and C. L. Yang, *J. Phys. Chem. C*, 2011, **115**, 4872–4878.
30 K. Suzuki, A. Kobayashi, S. Kaneko, K. Takehira, T. Yoshihara, H. Ishida, Y. Shiina, S. Oishic and S. Tobita, *Phys. Chem. Chem. Phys.*, 2009, **11**, 9850–9860.
31 C. J. Hawker and J. M. J. Frechet, *J. Chem. Soc., Chem. Commun.*, 1990, 1010–1013.
32 C. J. Hawker and J. M. J. Frechet, *J. Am. Chem. Soc.*, 1990, **112**, 7638–7647.
33 T. M. Miller, T. X. Neenan, R. Zayas and H. E. Bair, *J. Am. Chem. Soc.*, 1992, **114**, 1018–1025.
34 J. Hernando, J. P. Hoogenboom, E. M. H. P. van Dijk, J. J. García-López, M. Crego-Calama, D. N. Reinhoudt, N. F. van Hulst and M. F. García-Parajó, *Phys. Rev. Lett.*, 2004, **93**, 236404.
35 F. V. Bright and L. B. McGown, *Anal. Chem.*, 1986, **58**, 1424–1427.
36 J. R. Lakowicz, *Principles of Fluorescence Spectroscopy*, Springer, New-York, NY, 3rd edn, 2006.
37 M. Kasha, H. Rawls and M. A. El-Bayoumi, *Pure Appl. Chem.*, 1965, **11**, 371–392.
38 B. Valeur and G. Weber, *Photochem. Photobiol.*, 1977, **25**, 441–444.

